Supporting Information for

A Universal Strategy for Fabrication and Morphology Control of Polyoxometalate-Based Metal−Organic Frameworks

Xiao-Hui Li,‡ Yi-Wei Liu,‡ Ying Lu,* Zhong Zhang, Hong-Rui Tian, Shu-Mei Liu and Shu-Xia Liu*

Key Laboratory of Polyoxometalate Science of the Ministry of Education,

College of Chemistry, Northeast Normal University,

Changchun, Jilin 130024, China

*e-mail: liusx@nenu.edu.cn; luy968@nenu.edu.cn

Table of Contents

1. Experimental Details S3
2. Single-crystal structure of NENU-n S6
3. Characterization of original Cu substrates S6
4. Synthesis process of NENU-9 on Cu foil S7
5. UV-Vis measure of formed HPB S7
6. Characterization of as-synthesized NENU-9 on Cu foil S8
7. Thickness of NENU-9 on Cu foil S9
8. Schematic diagram of the formation process of NENU-n S10
9. Structure characterization of as-synthesized NENU-n encapsulating different POMs S11
10. Structure characterization of as-synthesized Cu-BDC on Cu foil S12
11. Particle size of NENU-9 synthesized on Cu foil S13
12. Morphology of NENU-n encapsulating different POMs S13
13. Morphology of NENU-9 produced at different reaction time S14
14. Characterization of NENU-9 produced on Cu wire at different reaction time S15
15. Characterization of NENU-9 produced on Cu powder at different reaction time S15
16. Characterization of NENU-9 produced on Cu mesh at different reaction time S15
17. Morphology of NENU-n produced with copper salt as the metal source S16

References S16

1. Experimental Procedures

Materials

All the raw chemicals were obtained commercially and used without additional purification. $H_4PVMo_{11}O_{40}$ ($PVMo_{11}$), $H_5PV_2Mo_{10}O_{40}$ (PV_2Mo_{10}), $H_6PV_3Mo_9O_{40}$ (PV_3Mo_9), $H_4SiMo_{12}O_{40}$ ($SiMo_{12}$), $H_3PMo_{12}O_{40}$ (PMo_{12}), $H_5SiVMo_{11}O_{40}$ ($SiVMo_{11}$) and $Cu_3(BTC)_2$ were synthesized according to the procedure described in the literatures[1-4] and characterized by FTIR spectra (Fig. S5 and S11a).

Characterization

Fourier transform infrared (FTIR) spectra were recorded in the range 400-4000 cm^{-1} on an Alpha Centaurt FTIR spectrophotometer using KBr pellets. Powder X-ray diffraction (PXRD) measurements were performed on a Rigaku Smartlab system with Cu Kα radiation in the angular range 2θ 5°-60° at 293 K. Scanning electron microscope (SEM) images were collected using a HITACHI SU8010 scanning electron microscope. UV-Vis spectra were recorded with a UV-6100 Double Beam spectrophotometer. Hiden isochema IGA 100B instrument was used to measure N_2 sorption at 77 K. The thickness of the crystalline NENU-9 layers growing on Cu foil was measured through subtracting the thickness of Cu foil from that of whole material (NENU-9 layers together with Cu substrate) by a digital caliper. Elemental analyses for Cu, P, Si and Mo were determined using a Leaman inductively coupled plasma (ICP) spectrometer.

Synthesis of NENU-9 on Cu foil

In a typical experiment, PV_2Mo_{10} (0.4 g, 0.16 mmol) was dissolved in 3 mL distilled water (solution A). H_3BTC (0.28 g, 1.33 mmol) was dissolved in 12 mL ethanol (solution B). A solution and B solution were uniformly mixed, then 20% NaOH aqueous solution (40 μL) was added into the mixed solution with continuous stirring to prepare the precursor solution. The precursor solution and a Cu foil (1 cm × 1 cm × 20 μm) were then sealed in a Teflon-lined autoclave and heated at 100 °C for rated time, followed by cooling to room temperature. Then solution was removed and the product was dried in air.

Synthesis of NENU-n encapsulating different Keggin-type POMs on Cu foil

$SiMo_{12}$ (0.4 g), $SiVMo_{11}$ (0.4 g), PV_3Mo_9 (0.4 g), $PVMo_{11}$ (0.4 g) and PMo_{12} (0.4 g) were respectively dissolved in 3 mL distilled water. The subsequent process was the same as the synthesis of NENU-9 on Cu foil. After reacting at 100 °C for 1 h, the corresponding products were obtained separately.

Synthesis of cubic NENU-9 on Cu wire

The process was similar to the synthesis of NENU-9 on Cu foil, but a Cu wire (1 cm length, 200 μm diameter) was immersed in the precursor solution. After reacting at 100 °C for 30 min, cubic NENU-9 crystals growing on Cu wire were obtained.

Synthesis of cubic NENU-9 on Cu mesh

The process was similar to the synthesis of NENU-9 on Cu foil, but Cu mesh (50 μm wire diameter, about 75 μm holes) was immersed in the precursor solution. After reacting at 100 °C for 2 h, cubic NENU-9 growing on Cu mesh was obtained.

Synthesis of cubic NENU-9 on Cu powder

The process was similar to the synthesis of NENU-9 on Cu foil, but Cu powder (200 mesh, 0.2 g) was immersed in the precursor solution. After reacting at 100 °C for 30 min, cubic NENU-9 was obtained.

Synthesis of Cu-BDC on Cu foil

PV_2Mo_{10} (0.2 g, 0.08 mmol) was dissolved in 5 mL distilled water (solution A). H_2BDC (0.1 g, 0.6 mmol) was dissolved in 10 mL DMF (solution B). A solution and B solution were uniformly mixed, and then 20% NaOH aqueous solution (80 μL) was added into the mixed solution with continuous stirring. Then a precursor solution was obtained after removing precipitation by filtration. The precursor solution and a Cu foil (1 cm × 1 cm × 20 μm) were then sealed in a Teflon-lined autoclave and heated at 100 °C for 12 h, followed by cooling to room temperature. Then solution was removed and the product was washed with ethanol and dried in air.

Synthesis of NENU-n with copper salt as the metal source

In a typical experiment, PV_2Mo_{10} (0.4 g, 0.16 mmol) and $Cu(NO_3)_2 \cdot 3H_2O$ (0.4 g, 1.7 mmol) were was dissolved in 3 mL distilled water and then 20% NaOH aqueous solution (60 μL) was added to prepare the solution A. H_3BTC (0.28 g, 1.33 mmol) was dissolved in 12 mL ethanol (solution B). Solution B was added into solution A with continuous stirring to prepare the precursor solution. The precursor solution was then sealed in a Teflon-lined autoclave and heated at 100 °C

for 1 h. Then NENU-9 was obtained after cooling to room temperature. Other NENU-n crystals were prepared by the same method but different POMs.

2. Single-crystal structure of NENU-n

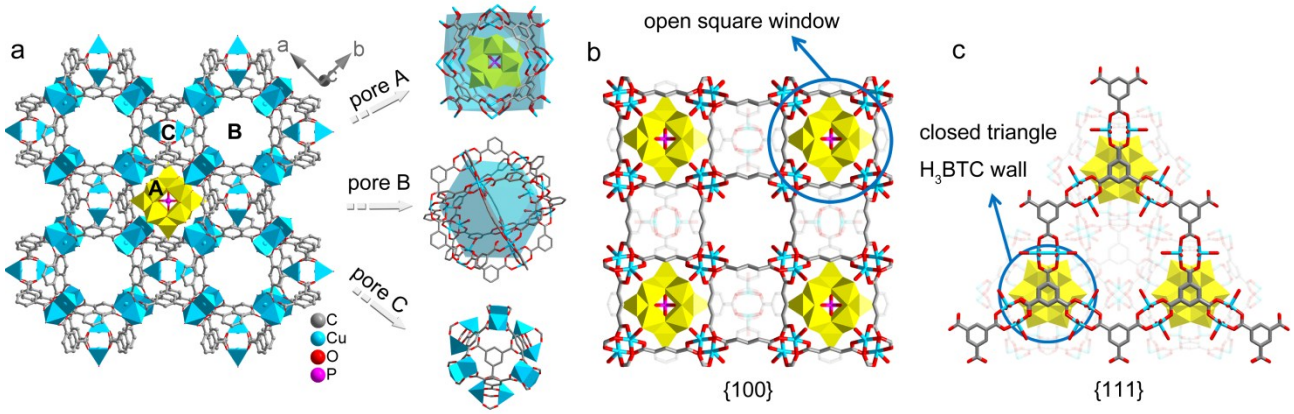

Fig. S1 (a) The structure diagram of NENU-n with three kinds of pores. (b) The surface structure of {100} facets with open square windows and (c) the surface structure of {111} facets with closed triangle H_3BTC walls in NENU-n.

As reported in our previous work,[5, 6] NENU-n, formulated as $[Cu_{12}(BTC)_8(H_2O)_{12}][H_nXV_xM_{12-x}O_{40}]$ (X = Si, Ge, P, As; M = W, Mo; x = 0, 1, 2, 3), are a series of crystalline compounds made up of $Cu_3(BTC)_2$ as the scaffold and encapsulating a Keggin-type POM in each pore A of $Cu_3(BTC)_2$ scaffold. There are three kinds of pores in the framework (pore A, B and C). Pore A has a larger free diameter (13 Å) and narrower square window (10 Å) which can fitly encapsulate a Keggin-type POM molecule (10.4 Å diameter). Thus, leaching out of the POM from the pore A of NENU-n is difficult. Pore B (10 Å) and pore C (5 Å) form channels that can be used for the transport of substrates in catalysis.

3. Characterization of original Cu substrates

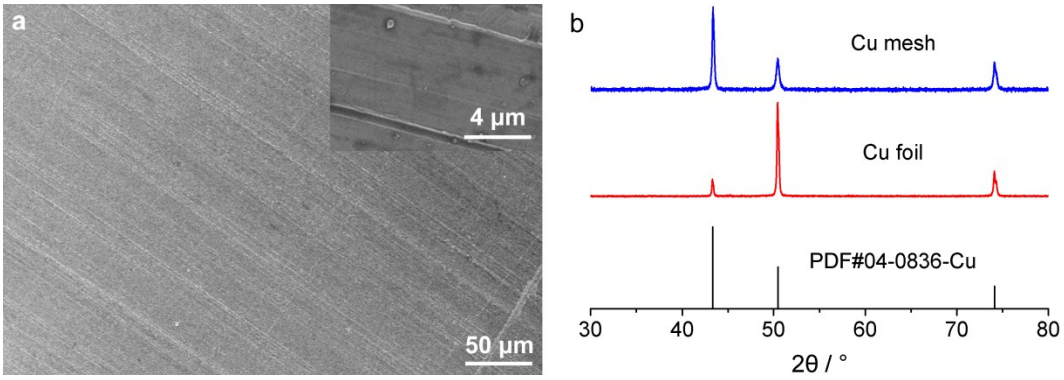

Fig. S2 (a) SEM images of original Cu foil. (b) PXRD patterns of simulated Cu and original Cu substrates (Cu foil and Cu mesh).

4. Synthesis process of NENU-9 on Cu foil

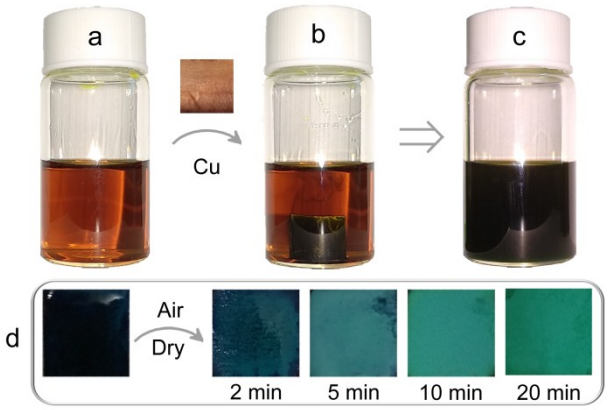

Fig. S3 The synthesis process of NENU-9 on Cu foil. (a) Photograph of the precursor solution prepared by mixing PV_2Mo_{10} aqueous solution and ethanol solution of H_3BTC. (b) Photograph of the solution just after a Cu foil was immersed in. (c) The solution after reacting for 1 h at 100 °C. (d) Drying process of the synthesized NENU-9 on Cu foil in air.

5. UV-Vis measure of formed HPB

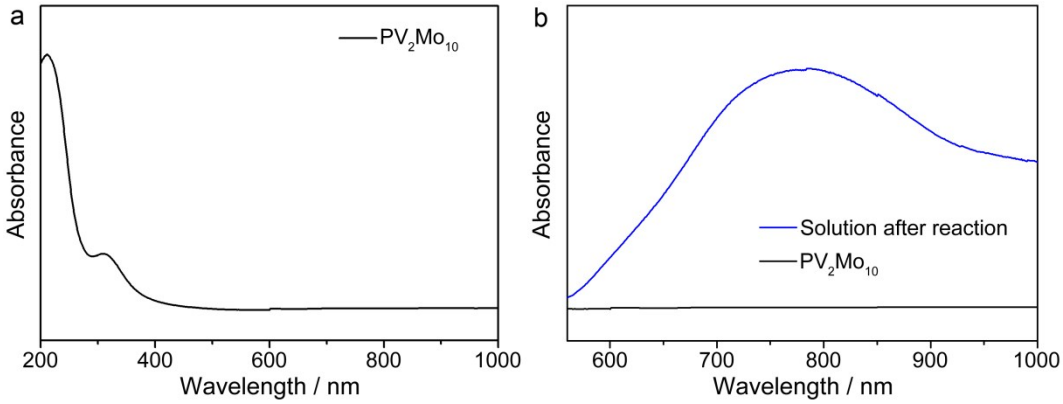

Fig. S4 UV-Vis spectrum of (a) PV_2Mo_{10} in the mixed solution of ethanol and water (v:v = 4:1) and (b) the solution after the fabrication reaction of NENU-9 proceeded for 1 h.

A broad peak centered at ~780 nm was appeared in the UV-Vis spectrum of the solution after the fabrication reaction of NENU-9, which is a characteristic peak belong to HPB,[7] indicating the formation of HPB in during the preparation of NENU-9.

6. Characterization of as-synthesized NENU-9 on Cu foil

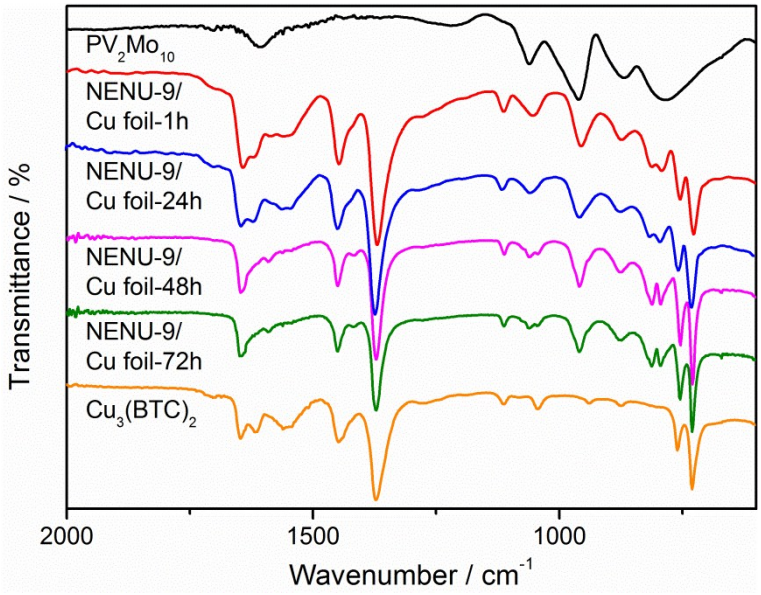

Fig. S5 FTIR spectra of PV_2Mo_{10} and as-synthesized NENU-9 on Cu foil.

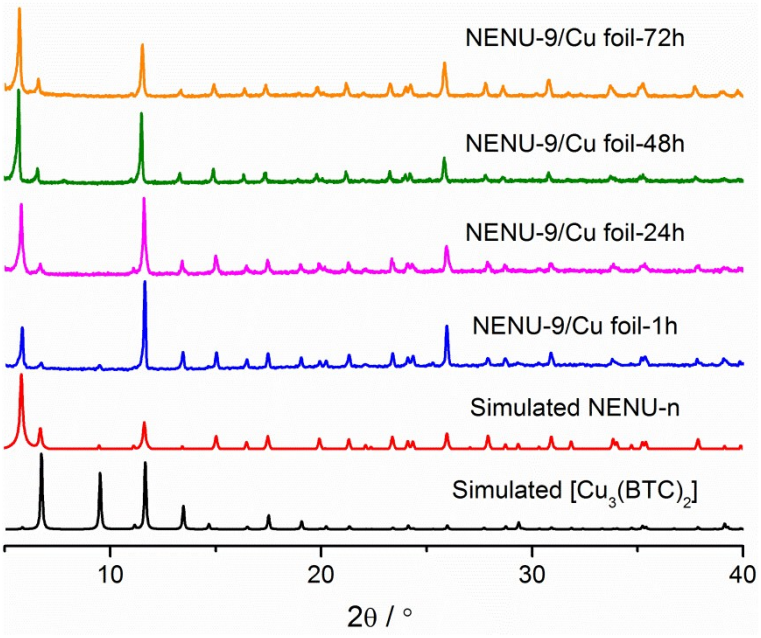

Fig. S6 PXRD patterns of as-synthesized NENU-9 on Cu foil and simulated NENU-n (the data of NENU-n crystal was obtained from our previous work[5]).

The IR characteristic peaks of Keggin-type POMs in the range of 600-1100 cm^{-1} indicated the encapsulation of POMs in $Cu_3(BTC)_2$ scaffold. The PXRD peak at $2\theta = 9.5°$ is a characteristic diffraction peak to distinguish whether there is $Cu_3(BTC)_2$ framework unloading POM.[6] No peak at $2\theta = 9.5°$ was observed in the PXRD patterns of materials prepared on Cu foil at 100 °C, indicating that there was no $Cu_3(BTC)_2$ unloading POM. In addition, the ratio of Cu:P:Mo for NENU-

9 was 12:1:10 as determined by ICP analysis (Table S1), which was consistent with the molecular formula of NENU-9 ($[Cu_{12}(BTC)_8(H_2O)_{12}][H_5PV_2Mo_{10}O_{40}]$). All these results proved the generation of pure phase NENU-9.

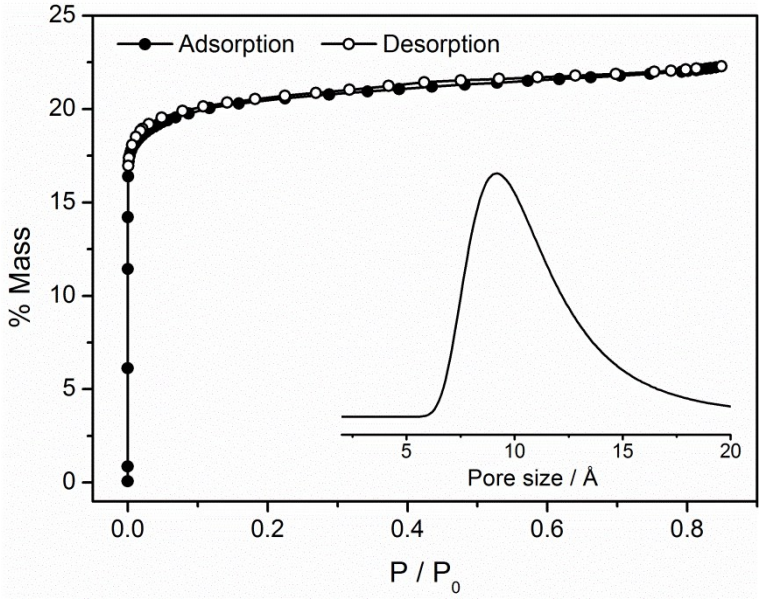

Fig. S7 N_2 sorption isotherms and pore size distribution of as-synthesized NENU-9 on Cu foil at 100 °C for 1 h.

N_2 sorption analysis of as-synthesized NENU-9 manifested the microporosity with a pore size of 9 Å and a BET surface area of 549 $m^2 g^{-1}$, which were close to the values of previously reported NENU-9.[6]

7. Thickness of NENU-9 on Cu foil

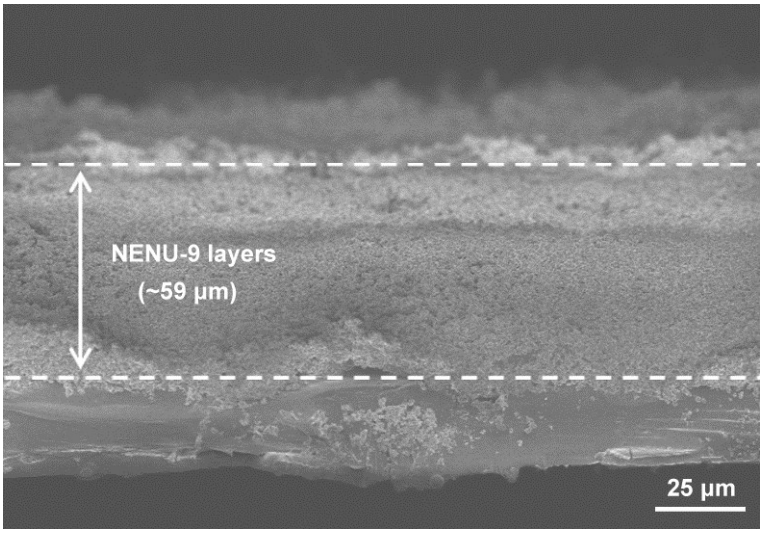

Fig. S8 Cross-sectional SEM image of synthesized NENU-9 on Cu foil at 100 °C for 1 h.

After reacting at 100 °C for 1 h, the thickness of the crystalline NENU-9 layers growing on Cu foil was about 59 μm as shown in cross-sectional SEM image, which was consistent with the result that measured through subtracting the thickness

of Cu foil from that of the whole material (NENU-9 layers together with Cu substrate) by a digital caliper (60 μm). The thickness of NENU-9 layers prepared at 100 °C for longer time was only measured by a digital caliper due to the significant fragility of thick crystal layers.

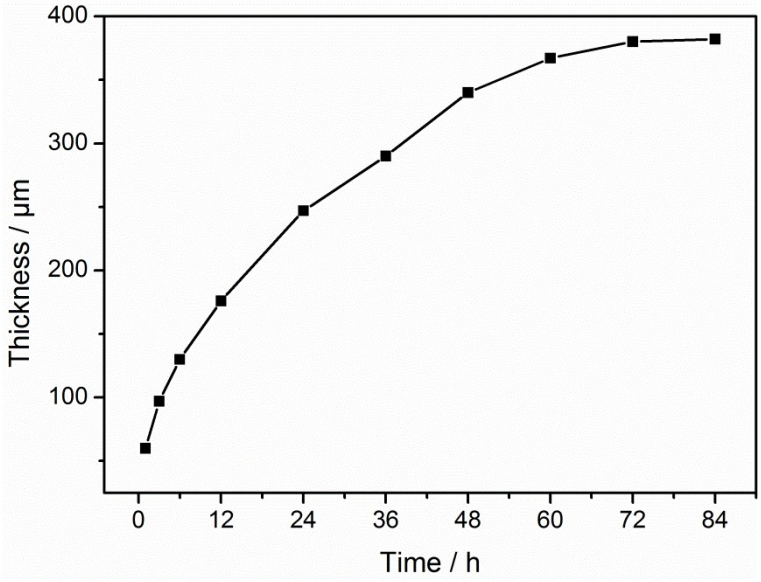

Fig. S9 The thickness of NENU-9 produced on Cu foil at 100 °C for different reaction time.

8. Schematic diagram of the formation process of NENU-n

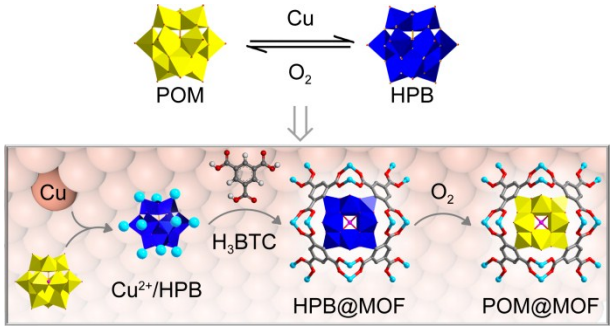

Fig. S10 Schematic diagram of the formation process of NENU-n by utilizing the oxidization of POMs to Cu.

9. Structure characterization of as-synthesized NENU-n encapsulating different POMs

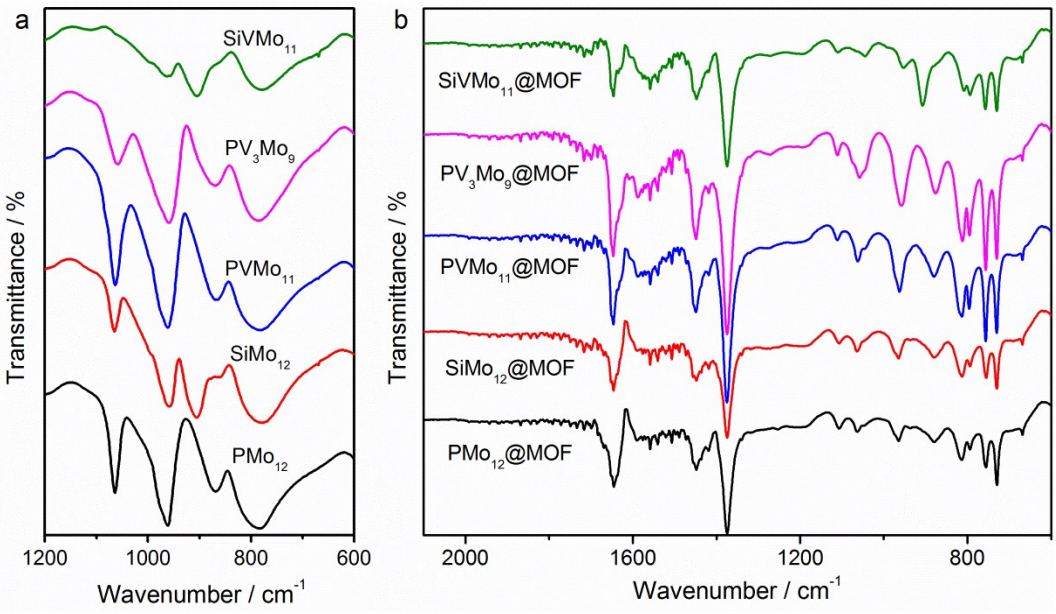

Fig. S11 FTIR spectra of (a) as-synthesized Keggin-type POMs with different negative charges and (b) corresponding POM@MOFs.

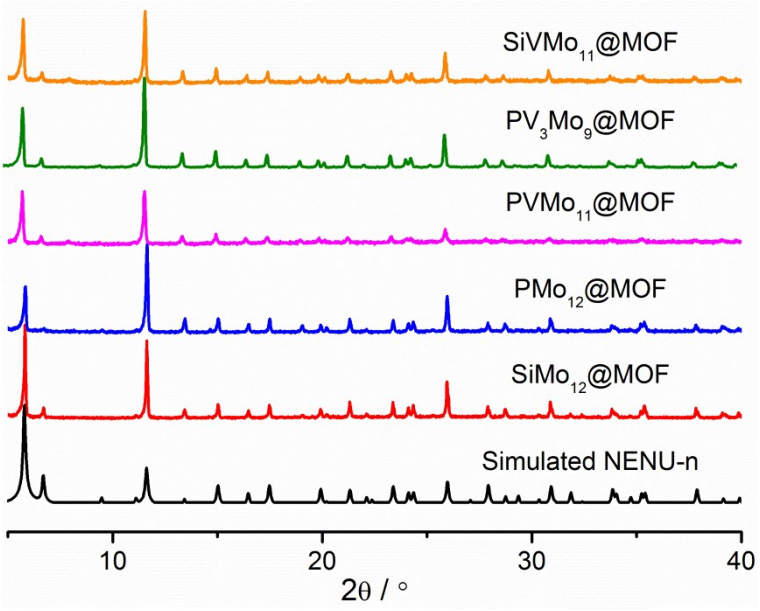

Fig. S12 PXRD patterns of NENU-n encapsulating Keggin-type POMs with different negative charges and simulated NENU-n.

Table S1 The element contents of as-synthesized NENU-n by ICP analysis.

Sample	n_{Cu} / μmol mL^{-1}	n_P / μmol mL^{-1}	n_{Si} / μmol mL^{-1}	n_{Mo} / μmol mL^{-1}	Cu:P(Si):Mo
PMo_{12}@MOF	0.907	0.075	--	0.901	12:1:12
$SiMo_{12}$@MOF	0.616	--	0.050	0.619	12:1:12
$PVMo_{11}$@MOF	0.672	0.056	--	0.615	12:1:11
PV_2Mo_{10}@MOF	0.835	0.070	--	0.692	12:1:10
PV_3Mo_9@MOF	0.979	0.082	--	0.739	12:1:9
$SiVMo_{11}$@MOF	0.695	--	0.057	0.637	12:1:11

Similar to the results of NENU-9, FTIR spectra of as-synthesized NENU-n indicated the encapsulation of POMs in $Cu_3(BTC)_2$ scaffold. All samples were detected by PXRD and there were no peaks at $2\theta = 9.5°$, indicating the pure-phase NENU-n. In addition, the ratio of POM-to-MOF for all synthesized NENU-n was determined by ICP analysis. The results showed that the molar ratio of Cu:P (or Si) was all 12:1, which is consistent with the molecular formula of NENU-n, further proving the generation of pure phase NENU-n.

10. Structure characterization of as-synthesized Cu-BDC on Cu foil

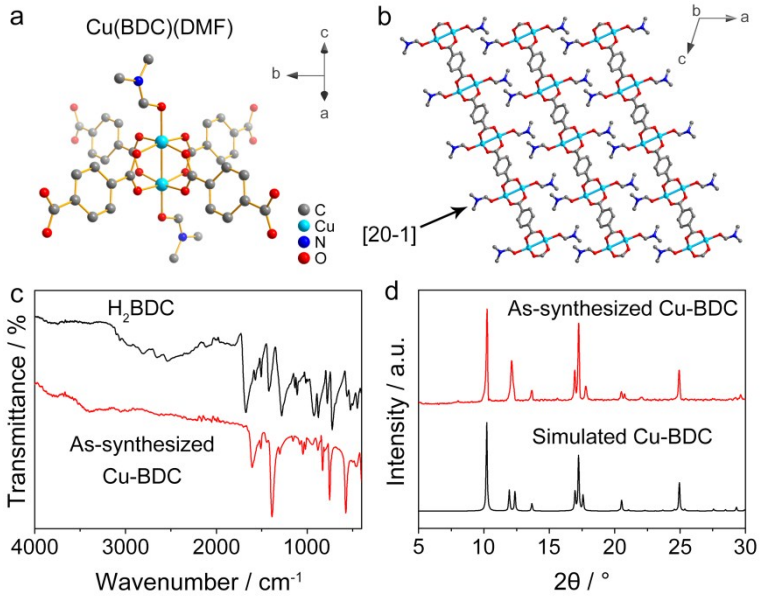

Fig. S13 (a) The structure diagram of dicopper paddle-wheel building unit in Cu-BDC. (b) The stacking of lamellar structures of Cu-BDC along [20-1] axis. (c) FTIR spectra of H_2BDC and as-synthesized Cu-BDC on Cu foil. (d) PXRD patterns of as-synthesized Cu-BDC on Cu foil and simulated Cu-BDC (the data of Cu-BDC crystal was obtained from the reported work[8]).

Cu-BDC ([Cu(BDC)(DMF)], H_2BDC = 1,4-benzenedicarboxylic acid) is composed of Cu^{II} atoms coordinating with

BDC linkers on {20-1} crystallographic planes to form 2D layers with a interlayer distance of 5.2 Å. In this system, POM is unlikely to be loaded in synthesized Cu-BDC due to the larger diameter of POM (10.4 Å). Thus, a pure Cu-BDC was formed, as confirmed by FTIR spectra and PXRD patterns.

11. Particle size of NENU-9 synthesized on Cu foil

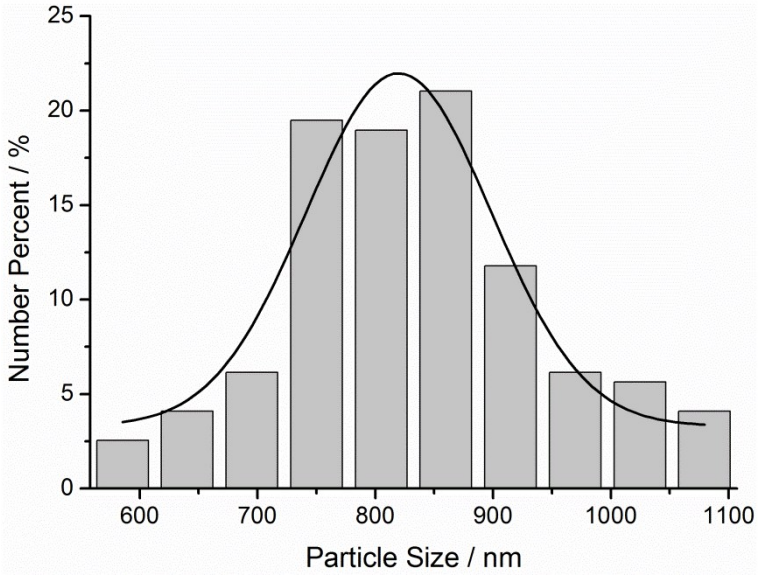

Fig. S14 Particle size analysis of NENU-9 crystal synthesized on Cu foil at 100 °C for 1 h.

12. Morphology of NENU-n encapsulating different POMs

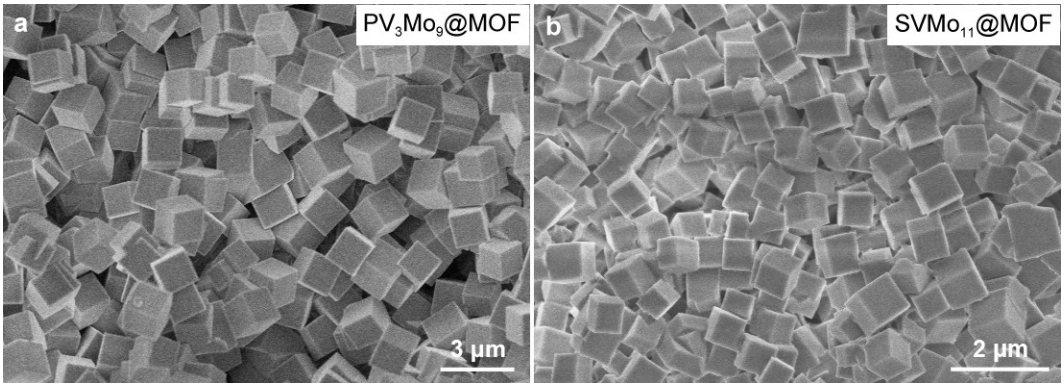

Fig. S15 SEM images of (a) PV_3Mo_9@MOF and (b) $SiVMo_{11}$@MOF.

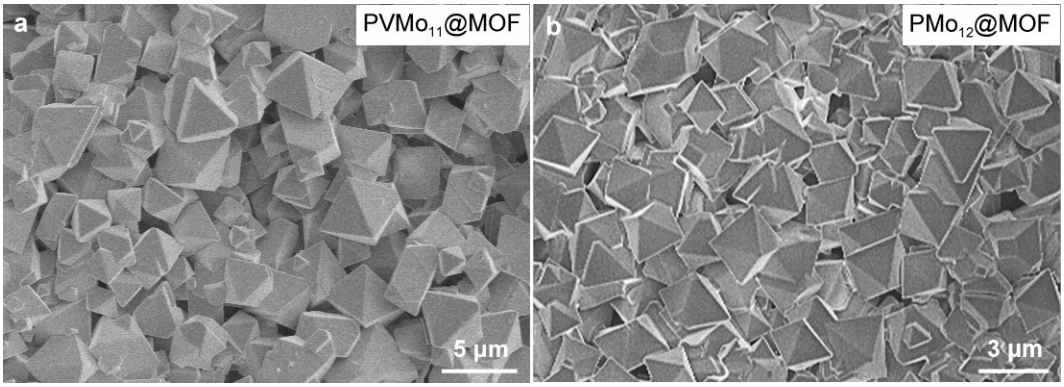

Fig. S16 SEM images of (a) $PVMo_{11}$@MOF and (b) PMo_{12}@MOF.

13. Morphology of NENU-9 produced at different reaction time

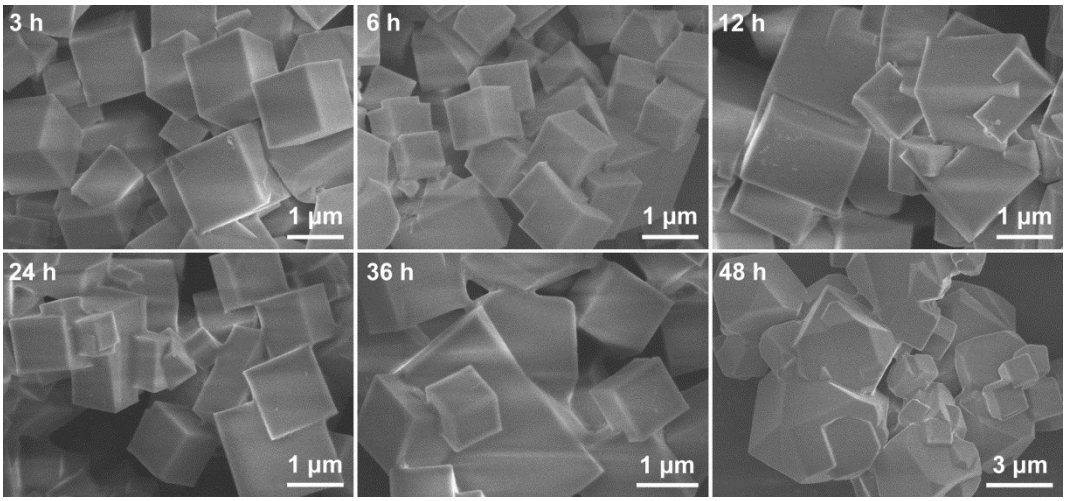

Fig. S17 SEM images of NENU-9 produced on Cu foil at 100 °C for different reaction time.

As the reaction time increased, the thicker NENU-9 layer was formed, even a thickness of hundreds micrometer. The large thickness and poor conductivity of NENU-9 made the sample particles easily flying by electron beams and pictures unclear during the SEM test. We used a conductive adhesive to paste the sample on the surface of NENU-9 layer at different reaction times and then the conductive adhesive was pasted on the sample stage for testing. Therefore, the morphology of NENU-9 on top was clearly detected and a morphologic change from cube to cuboctahedra was observed after 48 h.

14. Characterization of NENU-9 produced on Cu wire at different reaction time

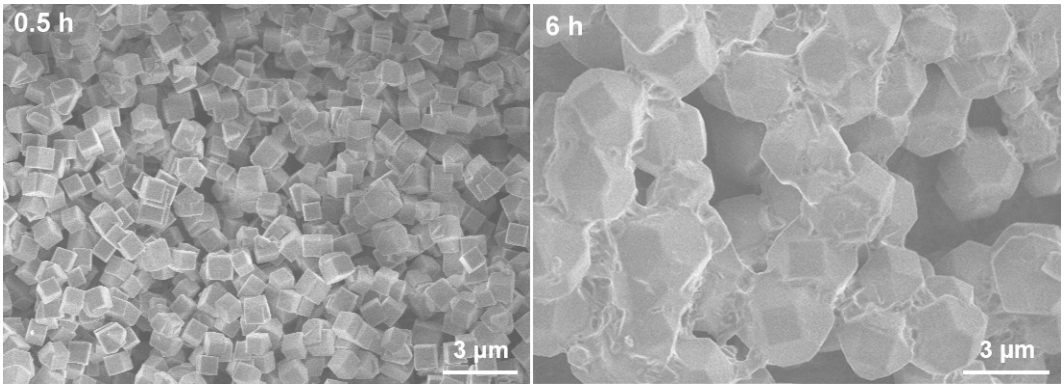

Fig. S18 SEM images of NENU-9 obtained on Cu wire within 0.5 h and 6 h.

15. Characterization of NENU-9 produced on Cu powder at different reaction time

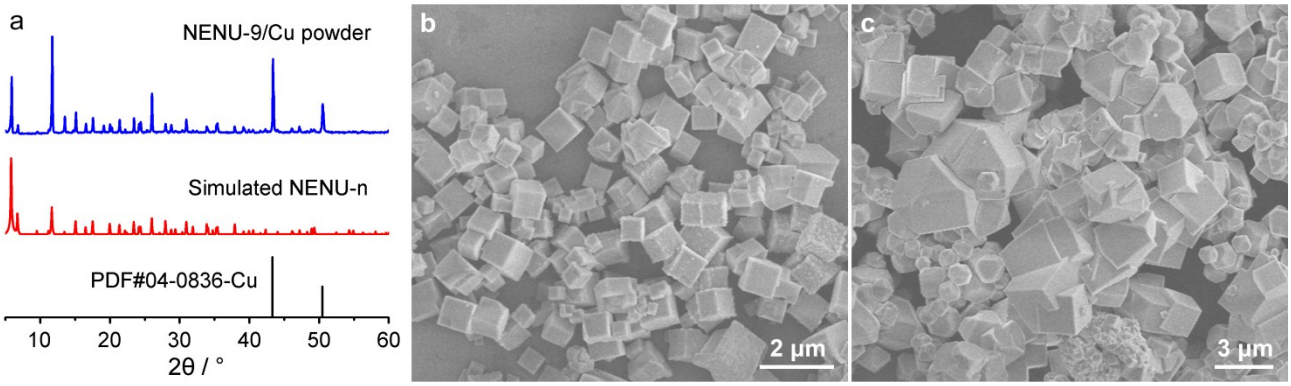

Fig. S19 (a) PXRD patterns NENU-9 obtained on Cu powder within 0.5 h. (b, c) SEM images of NENU-9 obtained on Cu powder within 0.5 h (b) and 6 h (c).

16. Characterization of NENU-9 produced on Cu mesh at different reaction time

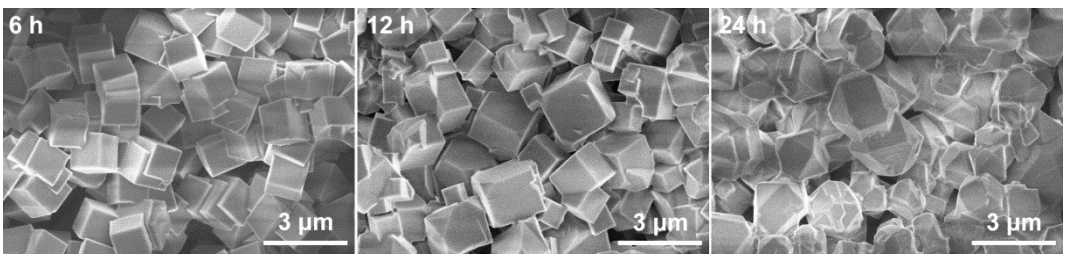

Fig. S20 SEM images of NENU-9 obtained on Cu mesh at different reaction time.

17. Morphology of NENU-n produced with copper salt as the metal source

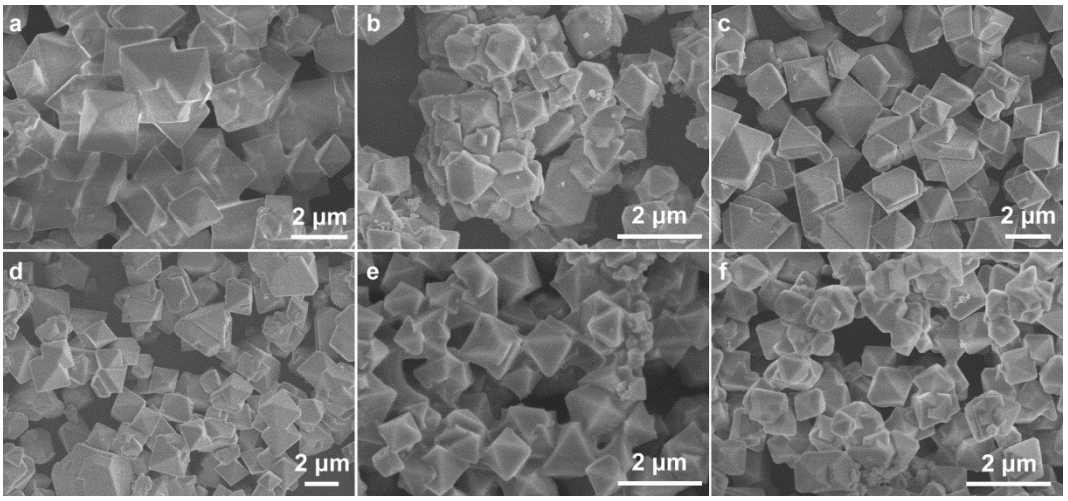

Fig. S21 SEM images of NENU-n obtained with $Cu(NO_3)_2$ as the metal source after reacting at 100 °C for 1 h. (a) $SiVMo_{11}$@MOF, (b) PV_3Mo_9@MOF, (c) PV_2Mo_{10}@MOF, (d) $PVMo_{11}$@MOF, (e) $SiMo_{12}$@MOF and (f) PMo_{12}@MOF.

References

1. G. A. Tsigdinos and C. J. Hallada, *Inorg. Chem.*, 1968, **7**, 437-441.
2. C. Rocchiccioli-Deltcheff, M. Fournier, R. Franck and R. Thouvenot, *Inorg. Chem.*, 1983, **22**, 207-216.
3. N. N. Chumachenko, R. I. Maksimovskaya, D. V. Tarasova, E. N. Yurchenko and I. V. Yaroslavtseva, *Kinet. Catal.*, 1984, **25**, 553-557.
4. S. S.-Y. Chui, S. M.-F. Lo, J. P. H. Charmant, A. G. Orpen and I. D. Williams, *Science*, 1999, **283**, 1148-1150.
5. C.-Y. Sun, S.-X. Liu, D.-D. Liang, K.-Z. Shao, Y.-H. Ren and Z.-M. Su, *J. Am. Chem. Soc.*, 2009, **131**, 1883-1888.
6. Y. Liu, S. Liu, S. Liu, D. Liang, S. Li, Q. Tang, X. Wang, J. Miao, Z. Shi and Z. Zheng, *Chemcatchem*, 2013, **5**, 3086-3091.
7. M. T. Pope, *Heteropoly and Isopoly Oxometalates*, Springer-Verlag, New York, 1983.
8. C. G. Carson, K. Hardcastle, J. Schwartz, X. Liu, C. Hoffmann, R. A. Gerhardt and R. Tannenbaum, *Eur. J. Inorg. Chem.*, 2009, 2338-2343.